Effects of Boundary Layer Dynamics and Meteorology on Ultrafine Particle Formation and Growth

Zachary Watson[1], Lee Tiszenkel[2], Arastoo Pour Biazar[3], Kevin Knupp[2,3], Shan-Hu Lee[2,3,*]

[1] Department of Meteorology, Florida Institute of Technology, Melbourne, Florida
[2] Department of Atmospheric and Earth Sciences, University of Alabama in Huntsville, Huntsville, Alabama
[3] Earth System Science Center, University of Alabama in Huntsville, Huntsville, Alabama

* Corresponding author (shanhu.lee@uah.edu)

Abstract. It is currently not well understood how the planetary boundary layer (PBL) dynamics affects the formation and growth of ultrafine particles in the atmosphere, because of the limited co-located aerosol size distributions and lidar measurements. Here we show, from long-term in-situ observations, a clear link between boundary layer processes and surface aerosol dynamics. Aerosol size distributions in the diameter range from 7-300 nm were measured with a scanning mobility particle sizer (SMPS) at the University of Alabama Huntsville campus in 2016, 2017, and 2022. The backscatter of larger aerosols was measured using a co-located lidar ceilometer. Meteorological surface parameters including temperature, relative humidity, station pressure, wind speed and direction, solar radiation, and precipitation were also measured. New particle formation (NPF) and long growth (over 12 hours) events occurred most frequently during the winter, unlike many other locations where NPF events occur more frequently in spring and fall, indicating that cooler temperatures play important roles in ultrafine particle formation in the warm subtropical environment. During the summer with strong solar radiation, there were more short-time growth events (less than 6 hours), likely associated with convection within the boundary layer. Our observations also show cold fronts affect the measured aerosol size distributions because the combination of precipitation scavenging and cleaner air can provide thermodynamic conditions favorable for NPF and aerosol growth. These results highlight the importance of meteorology on aerosol formation and growth.

Keywords:
Ultrafine particles, new particle formation, atmospheric dynamics, boundary layer, meteorology

1. Introduction

New particle formation (NPF) is the main source of ultrafine particles (UFP) in the atmosphere and contributes significantly to the global cloud condensation nuclei (CCN) production. Recent studies have shown how various chemical precursors, such as sulfuric acid, ammonia, amines, highly oxygenated organic molecules (HOMs), and iodide oxides can contribute to the formation and growth of new particles [1, 2]. Atmospheric dynamical processes such as storms, boundary layer processes, turbulence, and atmospheric waves can enhance NPF [3-10]. This is because these processes may produce high supersaturation ratios of water vapor in the atmosphere by rapidly mixing air masses with high humidity and low temperatures. Because nucleation is a non-linear process, even minor fluctuations in temperature and RH can increase nucleation rates over several orders of magnitude. Convection can also transport higher concentrations of nucleation precursors produced from the ground level into the free troposphere [21, 27-31]. Thus, the combination of colder temperatures, higher humidity, the lower surface area of preexisting aerosol particles, and higher precursor concentrations associated with convection can create an ideal condition for NPF in the free troposphere [30-32].

It is possible that new particles formed in the free troposphere can also be transported via downdrafts to the surface [6, 11-15]. For example, this downdraft process can serve as a main source of UFP in the Amazon rainforest where the local NPF does not occur, by "recycling" new particles formed in the cool free troposphere induced by biogenic nucleation precursors uplifted from the ground level [11, 12, 16]. Lai et al. [9] showed that vertical mixing within the boundary layer can also enhance NPF at the surface in polluted Northern China. Chen et al. [17] observed that ultrafine particles that were generated at the top region of the boundary layer are rapidly mixed throughout the boundary layer at the Southern Great Plains site in Oklahoma. Meskhidze et al. [18] suggested that large concentrations of particles freshly produced above the boundary layer can be brought to the surface by boundary layer growth and daytime mixing to become an important source of aerosol particles at the ground level at an urban site in North Carolina.

However, there are still very limited NPF studies that have detailed profiles of atmospheric boundary layer dynamics from in-situ observations; for example, most of the previous studies use the model-simulated boundary layer heights. Also, long-term measurements of simultaneous measurements of NPF and boundary layer dynamics are scarce. Here, we show long-term observations of aerosol size distributions, lidar ceilometer, and the ambient meteorological conditions in Huntsville, Alabama over four seasons to understand the link between the boundary layer dynamics and the surface UPF in the southeastern United States.

2. Methods

The measurement were made at the Severe Weather Institute and Radar & Lightning Laboratories (SWIRLL) building (https://www.nsstc.uah.edu/swirll/main/platforms/sfc.php) (34°43'29" N, 86°38'47" W, 212 m above mean sea level) at the University of Alabama in Huntsville (UAH) in Huntsville, Alabama. The aerosol sampling was taken from the roof of the SWIRLL building with the inlet 10 m above the ground. The lidar ceilometer and meteorology measurements were made at the surface.

Figure 1 shows the UAH and the surrounding Huntsville area. Huntsville has a population of 217,000 and is the largest city in the state of Alabama. The UAH campus is located approximately 10 km west of downtown Huntsville, 1 km north of Interstate highway 565 and 4.5 km to the east of US highway 231/431. The main industry in the region takes place in Decatur, located approximately 30 km to the southwest of UAH. There are also military exercises at Redstone Arsenal, about 10 km to the south of UAH.

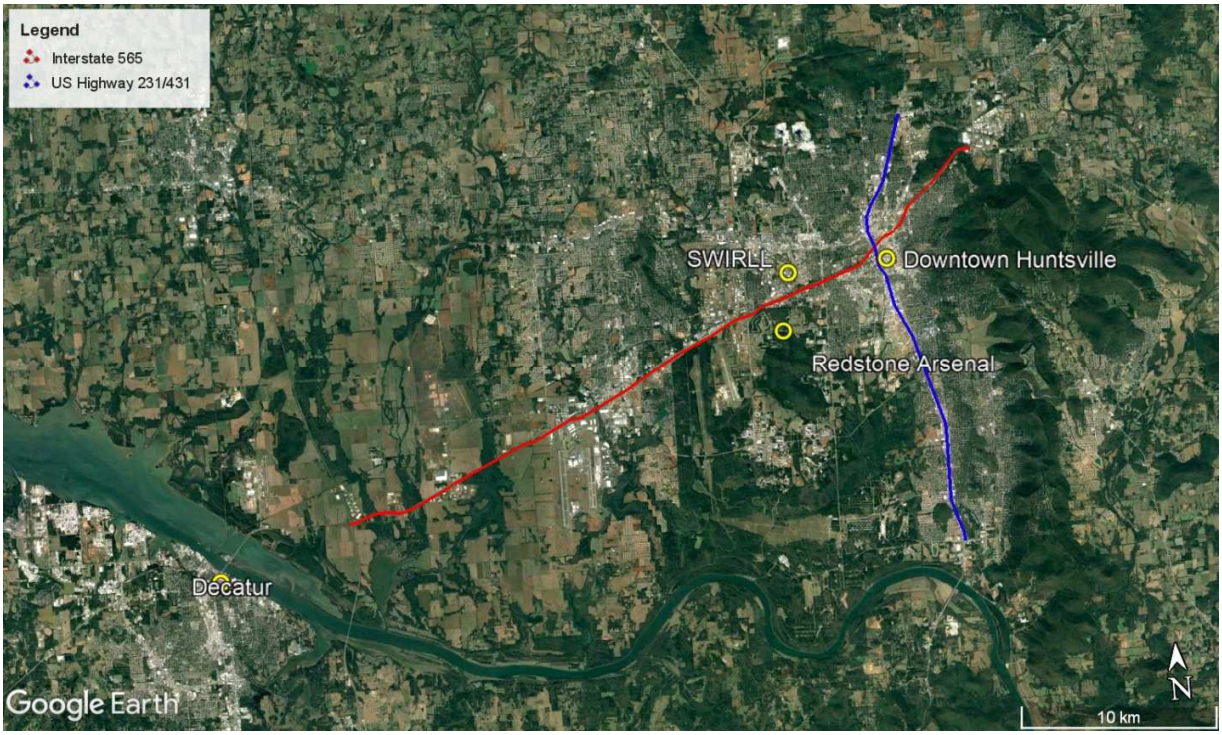

Figure 1. A Google Earth satellite imagery of the Huntsville area with labels showing the location of the measurement site at SWIRLL and probable sources of anthropogenic UFP. These sources include the highly traveled freeways of Interstate 565 (red line) and US Highway 231/431 (blue line), and locations such as Decatur, Alabama, Redstone Arsenal, and Downtown Huntsville, Alabama.

Aerosol size distributions in the diameter range of 7 to 300 nm were measured with a scanning mobility particle sizer (SMPS). The SMPS has two components: a differential mobility analyzer (DMA, TSI 3081) and a butanol-based condensation particle counter (CPC, TSI 3772). In this study, particles within the size range fro 7-300 nm were loosely defined as UFP. The UFP events were classified into two main categories: (1) UFP from NPF with characteristic "banana" shaped aerosol size distributions, and (2) UFP associated with sustained aerosol growth (typically longer than 12 hours), as discussed in the following section.

Growth rates (GR) were calculated based on the measured aerosol size distribution:

$$GR = \frac{dD_p}{dt} \approx \frac{D_f - D_i}{dt} \quad (1)$$

where dD_p is the change in median diameter from the beginning to the end of the growth event, D_i is the initial particle size, D_f is the final particle size, and dt is the length of the growth event. The standard deviations for GR (σ_{GR}) were determined using propagated error techniques. The standard deviation for the initial (σ_{Di}) and final (σ_{Df}) particle sizes were calculated from the aerosol size distribution, and the accuracy of the estimation of event length was 15 minutes (σ_{dt}). The propagated error formula for GR based on Equation 1 is:

$$\sigma_{GR} = \sqrt{\frac{(dt)^2(\sigma_{Df}{}^2+\sigma_{Di}{}^2)+\sigma_{dt}{}^2(D_f-D_i)^2}{(dt)^4}} \quad (2)$$

where $D_{p\text{-}i}$ and $D_{p\text{-}f}$ are the initial and final median particle diameters; $\sigma_{Dp\text{-}i}$ and $\sigma_{Dp\text{-}f}$ are the standard deviations of the initial and final particle diameters.

A Vaisala CL51 lidar ceilometer was used to obtain aerosol backscatter profiles. The lidar has a wavelength of 910 nm and has a vertical range from 0-15 km, detecting up to three cloud bases. The purpose of using backscatter profiles obtained from the ceilometer was to identify the planetary boundary layer (PBL) height, as well as the presence of clouds and rain fall events. This study will focus on 0-4 km backscatter profiles.

The surface meteorological were measured with a suite of instruments: Campbell Scientific 107 temperature probe for 2-meter air temperature, Vaisala HMP-45C temperature/relative humidity probe for 2-meter relative humidity, Vaisala PTB-210 barometer for station pressure, RM Young 05103 Wind Monitor for 10-meter wind speed and direction, Texas Instruments TR-525I rain gauge to track rainfall, and a Eppley Labs Pyranometer for solar radiation measurements.

Table S1 summarizes the measurement data of the SMPS, lidar ceilometer, and the surface meteorology parameters. The SMPS was active from 30 June 2016 to 14 April 2017, and from 1 January 2022 to 23 March 2022. In total, 199 days of data of SMPS measurements, crossing four seasons, are included in this study.

3. Results and Discussion

3.1. Overview and seasonality

For the seasonality analysis, we defined the seasons as the following: spring from March to May (MAM), summer from June to August (JJA), autumn form September to November (SON), and winter from December to February (DJF). Table 1 summarizes the seasonally averaged measurements of UFP concentrations in the diameter from 7 to 300 nm, NPF frequencies, overall GR, PBL heights, and 2 m air temperature.

Table 1. Summary of the measured aerosol and meteorology data averaged during different seasons. Numbers in parentheses correspond to the number of days of data available to calculate that particular average. Aerosol quantities are expressed with an error of one standard deviation (± 1σ). The overall mean values were calculated using a weighted average for each season, and the overall standard deviations were weighted by degrees of freedom of the seasonal standard deviations (sample size – 1).

Parameter	Winter (DJF)	Spring (MAM)	Summer (JJA)	Autumn (SON)	Overall

7-300 nm UFP Concentration (cm^{-3})	$(5.3\pm3.3) \times 10^3$ (58)	$(4.9\pm3.0) \times 10^3$ (47)	$(4.5\pm2.4) \times 10^3$ (44)	$(4.4\pm2.1) \times 10^3$ (50)	$(4.8\pm2.8) \times 10^3$ (199)
NPF Frequency (% of days)	24 (58)	26 (47)	11 (44)	12 (50)	19 (199)
Growth Rate ($nm\ hr^{-1}$)	2.2 ± 4.8 (12)	1.8 ± 5.0 (10)	1.2 ± 4.9 (1)	2.7 ± 3.9 (6)	1.7 ± 4.7 (29)
Daily Maximum PBL Height (m)	1450 ± 500 (27)	1550 ± 450 (32)	1800 ± 350 (34)	1900 ± 300 (35)	1700 ± 450 (128)
2m Air Temperature (°C)	8.0 ± 5.9 (57)	14.5 ± 4.8 (47)	27.7 ± 1.7 (35)	23.5 ± 4.1 (50)	17.4 ± 8.9 (189)

NPF events were most common in the spring (26%), then the winter (24%), autumn (12%), and least common in the summer (11%) (Table 1). Our results agree with previous studies that suggest NPF events are the most common in the spring, but disagree that NPF is the least common in the winter in many other locations [1, 2]. For example, from 4 years of long-term observations of NPF in Kent, Ohio, Kanawade et al. [19] showed that NPF was most common in the spring, then autumn, summer, with the least NPF events in winter. Our results suggest that low temperatures are especially important for NPF in the relatively warm climate in the sub-tropics. Previous studies have suggested that colder temperatures are more favorable for UFP formation [11] and high temperatures can cause evaporation of freshly nucleated particles [1].

Particle number concentrations also showed the similar seasonality, highest in the wintertime at $(5.3\pm3.3) \times 10^3$ cm^{-3} and lowest in the autumn at $(4.4\pm2.1) \times 10^3$ cm^{-3}. The number concentrations for all seasons can be seen in Table 1. This was likely due to the lower PBL heights seen during the colder weather. The height and dynamics of the PBL (especially convection) can affect surface aerosol dynamics, especially with respect to particle concentrations. The PBL height was estimated using the lidar ceilometer with larger heights typically associated with stronger convective and thermal mixing. Seasonally averaged temperature and PBL heights agreed quite well ($R^2 = 0.812$) where seasons with higher temperatures had higher PBL heights, although there was not as strong of a correlation between daily averaged temperature and daily maximum PBL height ($R^2 = 0.305$) since deep boundary layers can still develop in the wintertime when temperatures are cold (see Figures S1 and S2). During the summer and autumn, the PBL heights were at their highest (Table 1), so there was the most mixing and dilution of particles within the boundary layer. The summer and early autumn are associated with large amounts of solar radiation at the surface, leading to increased heating, which results in stronger thermals and convective mixing within the boundary layer. These processes both act to increase the boundary layer height, and tend to mix out and dilute the UFP concentration, which could also affect NPF initiation. On the other hand, during the wintertime, the boundary layers are at their lowest with weak thermals and mixing, so other particles were trapped near the surface, increasing the concentrations. Thus, due to lower temperatures and due to lower PBL heights, in overall, there were higher concentrations of UFP and higher NPF frequencies.

The average overall growth rate (during the entire growth period) of the median particle diameter during aerosol growth events in Huntsville was 1.7±4.7 nm hr^{-1} (Table 1) and had a range of 0.9 - 4.1 nm hr^{-1} (Table S2). In comparison, observations showed growth rates in Ozark Forest in Missouri ranged from 1.6 – 11.2 nm hr^{-1} (Yu et. al, 2014), in Ohio rates from 0.5 – 12 nm hr^{-1} (Kanawade et. al, 2012), and in North Carolina from 1.6 - 5.7nm hr^{-1} (Meskhidze et. al, 2019). Overall, the aerosol growth rates were slightly lower in Huntsville than at these locations (Table 1). The growth rates in the autumn were the largest (2.7 ± 3.9 nm hr^{-1}), followed by winter (2.2 ± 4.8 nm hr^{-1}), spring (1.8 ± 5.0 nm hr^{-1}), then summer (1.2 ± 4.9 nm hr^{-1}). Ambient temperature is also associated with NPF precursor emissions, e.g., with highest biogenic VOCs in the summer [20]. The fact that in summer, we still had lowest GR, emphasize the thermodynamics effects of lower temperatures on NPF. Compared to boreal forests in high latitudes with relatively lower temperatures year around, high emissions of monoterpenes in summer important for higher growth of new particles [2]. But at our subtropical site, it is likely that the thermodynamics effects due to higher temperatures overweigh stronger biogenic emissions in summer.

Most often, particles larger than 100 nm are considered as a CCN proxy, studies have shown that smaller particles (e.g., 60 nm or larger) can also act as CCN depending on chemical composition and atmospheric conditions [21, 22]. Of the growth events measured in Huntsville, only one of the 29 events (3%) resulted in a median particle diameter 100 nm or larger (Table S2); however, 15 of these growth events (52%) resulted in particles that grew to a median size of 60 nm or larger (Table S2). Across various locations globally, the percentage of NPF events that produce CCN-size particles range from approximately 10% to 60%, within the range previously reported [2].

There are two main UFP sources at urban sites, primary particles emitted from traffic and secondary NPF processes [23-26]. From the measured size distributions, however, we found that UFP concentrations during the rush hours were usually significantly lower than during NPF. Thus, at our site, perhaps because it is located at the university campus, the UFP was mainly from NPF rather than traffic emissions. A recent study also indicated that at urban sites, traffic can also emit sub-3 nm particles [27]; another study also suggested that oxygenated organics emitted from vehicle exhausts are largely responsible for urban NPF [28]. In this context, we note that of the 29 NPF events in Table S1, 8 (28%) of them occurred near the rush hours.

3.2. Effects of Meteorology on NPF Initiation

One type of meteorological event thought to be of great importance to NPF initiation in Huntsville, Alabama is a cold front passage. Out of the 29 NPF initiations reviewed in this study (Table S2), 22 of them occurred within 48 hours of a cold front passage (76%, Table S3). Only five NPF events took place with a PBL height greater than 1000 m and 11 events took place with a PBL height of 500 m or less.

Figure 2 shows the measured lidar ceilometer backscatter intensity, surface meteorological data, and aerosol size distributions on 29-30 December 2016 after a cold front passage at approximately 0600 UTC on 29 December. Extremely high lidar backscatter values (e.g., black color) are typically indicative of clouds and precipitation. Clouds can be seen from 0000-1000 UTC with precipitation from around 0300-0700 UTC on 29 December from Figure 2a. This period of precipitation was also observed by the surface station, as seen in Figure 2d. Shortly after the rainfall started, Figure 2e shows the UFP concentrations immediately decreased to significantly lower values. The backscatter in the lidar was also lower after the rain than it was before the rain, indicating that larger particles were also scavenged from

the PBL. These results indicate that precipitation scavenging may be an important process for creating a more favorable environment for NPF to occur.

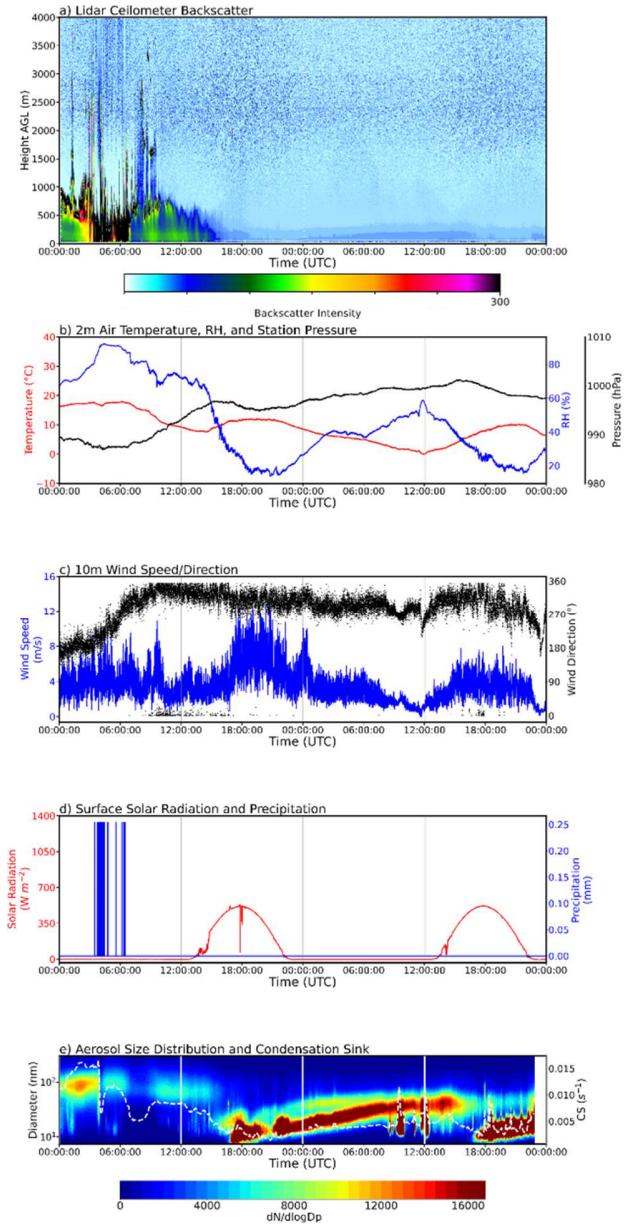

Figure 2. Meteorological and aerosol measurements for 29-30 December 2016 including a) lidar ceilometer backscatter intensity, b) 2 m air temperature in °C (red line), 2 m relative humidity (RH) in % (blue line), and station pressure in hPa (black line), c) 10 m wind speed in $m \cdot s^{-1}$ (blue line) and 10 m wind direction in degrees (black dots), d) solar radiation at the surface in $W \cdot m^{-2}$ and precipitation in mm, and e) 7-300 nm aerosol size distribution and condensation sink (CS) time series. All times are UTC. The local 06:00 and 18:00 are indicated as vertical bars.

The precipitation scavenging event discussed above was also associated with a cold front from a nearby low pressure system and associated advection of a modified maritime polar air mass, which acted to reduce the relative humidity, as seen in Figure 2b. Since rainfall typically occurs with both frontal and cyclone passages, precipitation scavenging may be an important factor favoring for NPF ahead of the front. There are several factors that make post-cold frontal air masses favorable for NPF and aerosol growth. First, the air behind the front is generally clean. We observed that precipitation scavenging occurring ahead of the front. There were relatively high backscatter values near the surface while the clouds were present, indicating larger particles present in the PBL. Around 1500 UTC, the backscatter decreased significantly, indicating a lack of large particles in the PBL, likely due to the advection of cleaner air into the region, as well as the development of a convective PBL on the afternoon of 29 December. There was a sudden decrease in ultrafine particle concentrations around 0400 UTC, just after the precipitation began, and a NPF event initiated near 1700 UTC, two hours after the backscatter decrease. At the time of NPF, the deep, dry, and vigorous mixing was occurring in the PBL, indicated by the low RH and gusty winds in Figures 2b and 2c, respectively.

The growth event continued past 0000 UTC into December 30, as a result of prolonged periods of low backscatter and a clean PBL (Figure 2). The initial growth event lasted until approximately 1500 UTC on 30 December. The concentrations of the resultant UFPs decreased, possibly due to dilution, and a new growth event initiated shortly after at around 1700 UTC. The conditions on 30 December appeared to be quite similar to the post-rain environment of the prior day with low RH and the development of a convective PBL.

Both NPF events occurred when RH was low, wind speeds were large and gusty (analog for high mixing), and near the daily peak of solar radiation, all shown in Figure 2. All of these meteorological parameters (except for the wind speed) during the NPF initiation follow what is expected from previous findings (e.g., [18]). The meteorological conditions were similar the next day, which supports why the aerosol dynamics behaved similarly. Cold fronts thus appear to provide a quite favorable environment for NPF to occur in Huntsville, Alabama. However, there were some cases where a cold front passage did not help to trigger a NPF initiation. A cold front passage occurred on 4 February, 2022, but there were no NPF initiations on 4-6 February, 2022 (Figure S3). The reason for this is not immediately clear and should be investigated in the future.

Another trend in the boundary layer is that NPF is unfavorable if the PBL is dominated by large particles. In Figure 2, the first NPF event did not initiate until after the lidar backscatter decreased, indicating the concentrations of relatively large particles had been reduced. Conversely, on 24 March 2017, the presence of large particles was detected by the ceilometer throughout the entire day (Figure 3a). In addition to the high backscatter near the surface, there was also a cloud layer beginning at 0600 UTC that followed the top of the PBL, and low backscatter values were found above the PBL. The lidar also shows the diurnal evolution of the PBL, suggesting vigorous mixing was occurring. The spring season is a very common time for pollen production by vegetation, particularly oak and other trees, in the southeastern US [26]. The high backscatter was likely caused by pollen being mixed in the PBL by the winds. The aerosol size distribution (Figure 3e) shows moderate concentrations of CCN sized particles until about 0800 UTC, but the concentrations start decreasing after this time. After about 1400 UTC, there were few UFP present (Figure 3e). A weak NPF and growth event tried to initiate around 1600 UTC, but the concentrations remained low throughout that entire event (Figure 3e).

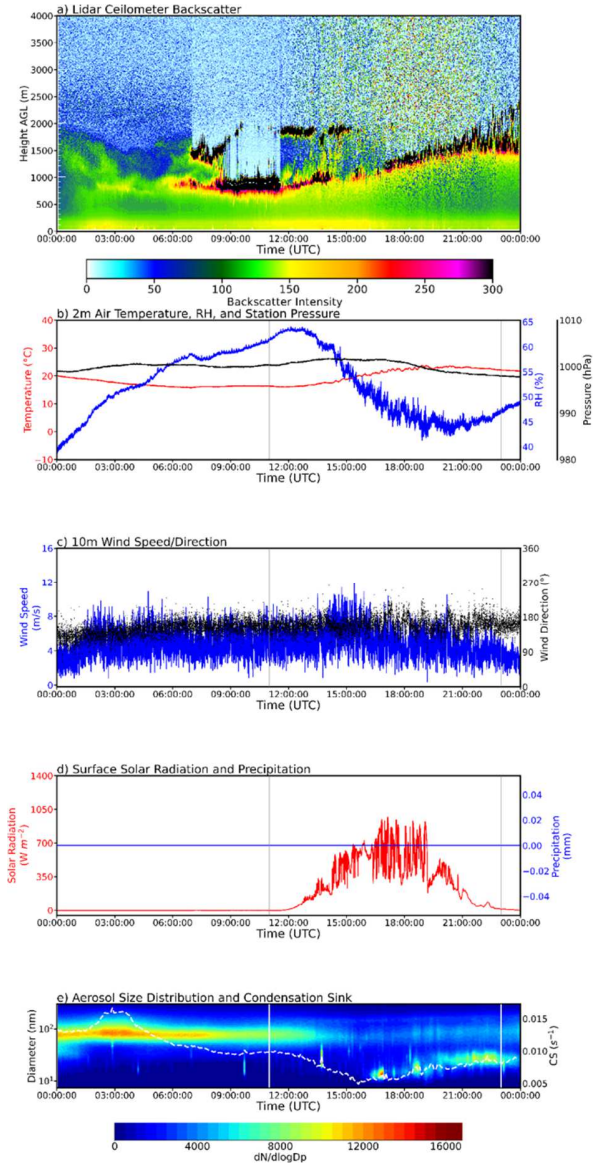

Figure 3. Same as Figure 2 but for 24 March 2017.

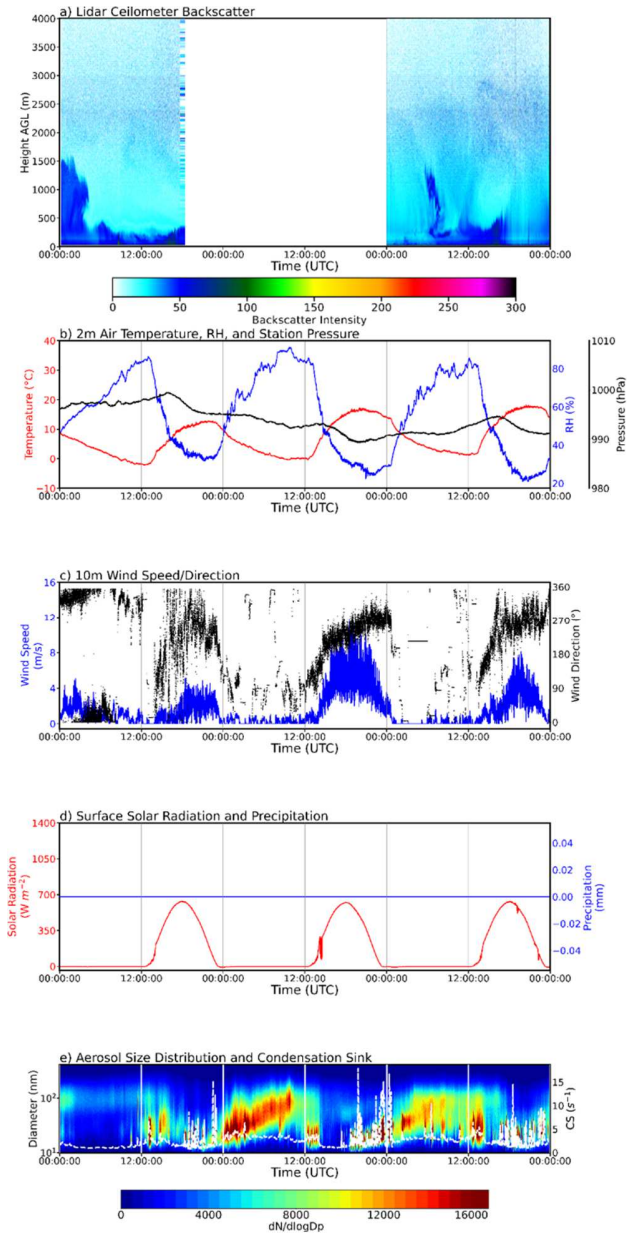

Figure 4. Same as Figure 2 but for 8-10 February 2022.

3.3. Sustained long-growth

Sustained particle growth events are defined as those that last for more than twelve hours. In Table S2, all but five of the NPF initiations resulted in a growth event that was shorter than twelve hours. The remaining 83% of NPF events resulted in these long growth events. These long growth events were the most common in the winter followed by the spring, similar to the NPF frequency. During both of these season, and the spring in particular, there were several back-to-back days of NPF and growth events taking place. The longest of these events was three days of repeated growth events on 8-10 February 2022 (Figure 4). These long growth events were typically associated with the clean, cool airmasses after a cold front passage as indicated by the reduction in lidar backscatter at 1700 UTC (Figure 4a). The

temperatures were unseasonably warm with clear skies and afternoon RH values near 25% (Figure 4b) are all indicative of a convective boundary layer with vigorous mixing. The initiation of the NPF events near 1800 UTC (Figure 4e) coincide with the reduction in lidar backscatter (Figure 4a) and an increase in the wind speed and gusts (Figure 4c), which both suggest vigorous mixing within the PBL, similar to the case in Figure 2. The maximum frequency of cold fronts and the presence of cold air masses in the winter can help to explain the high amount of long aerosol growth events.

Even though the wintertime was seen to have lower PBL heights and higher UFP number concentrations, on average (Table 1), in this case, the PBL was more vigorous than normal for this time of year. Instead of seeing UFPs trapped near the surface, convective mixing acted to dilute them, a feature more common in summertime PBLs. Additionally, on 10 February 2022, there are rapid changes in the concentration of UFPs at the surface. Since there is not much dilution, this could be a case where non-local mixing and thermals dominate vertical transport within the PBL [26].

In the cases shown in Figure 2 and Figure 4, NPF and long growth events were associated with both deep PBLs and cool temperatures associated with synoptic scale weather disturbances. Figure 5 shows lidar backscatter, surface measurements and aerosol size distribution for 30 June 2016. Similar to the other cases, Figure 5a shows the PBL height was approximately 2000m at 2100 UTC (although solar radiation contamination reduces the confidence in this estimate) and the RH decreased to near 25%, indicative of strong mixing (Figure 5b). The aerosol size distribution in Figure 5e also showed a growth event that initiated in the previous day that gradually ended (possibly due to dilution) at approximately 1700 UTC, similar to 30 December 2016 and 10 February 2022 in Figure 2e and Figure 4e; however, in this case, there was no initiation of NPF in the afternoon. The main difference is that the temperatures are much higher in Figure 5b (about 30°C) than in Figure 2b or Figure 4b (both are about 10°C). This could be a result of high temperatures contributing to the thermodynamic instability of freshly nucleated UFPs.

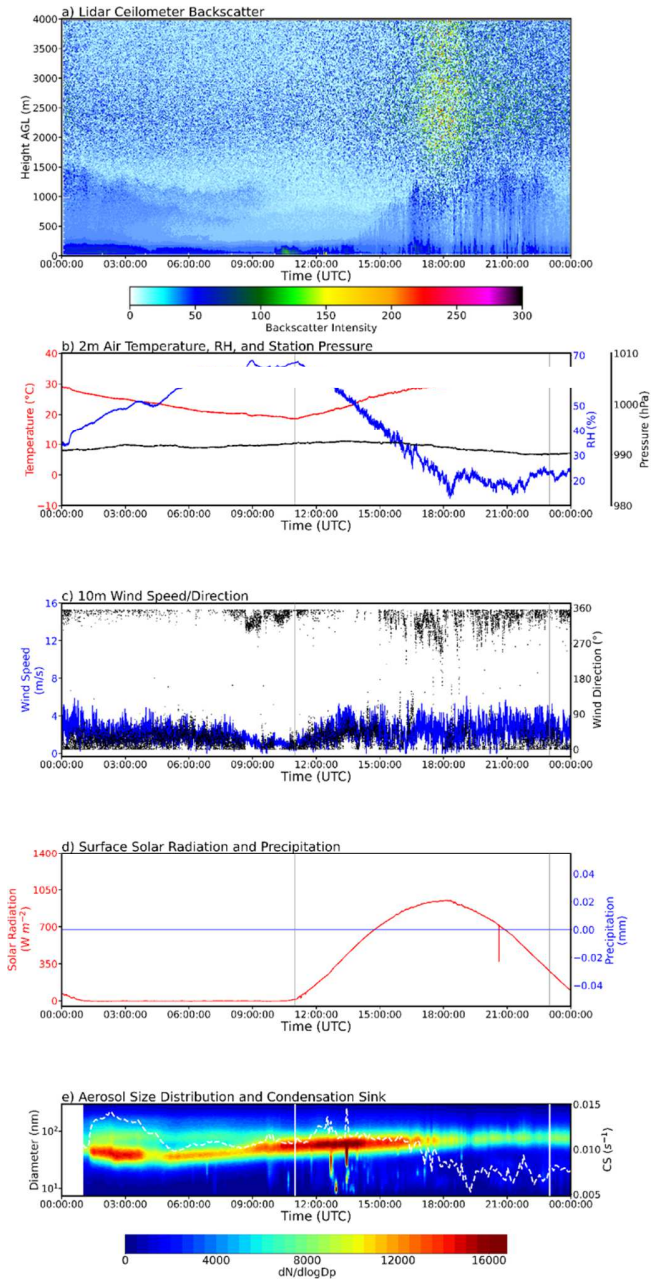

Figure 5. Same as Figure 2 but 30 June 2016.

4. Conclusions

From long-term measurements of 0-4 km lidar ceilometer backscatter profiles, surface meteorology parameters, and aerosol size distributions in the southeastern US, we identified cases where meteorology had a significant impact on the surface aerosol dynamics. The most important meteorological event was cold front passages. There were consistent patterns of NPF followed by long aerosol growth events that were initiated several hours after the occurrence of precipitation scavenging and cooler, cleaner air moving into the region behind the front. Other meteorological events thought to

have an impact are the boundary layer heights, convective mixing, and cloud-aerosol interactions near the top of the boundary layer. NPF events occurred most frequently in the winter and least frequently in the summer, indicating that low temperatures are important for NPF in warm climates such as in the southeastern US.

Acknowledgements

This research is supported by NSF (AGS-2209722). Zachary Watson was a participant of the NSF REU program at UAH (AGS-1757892).

References:

1. Lee, S.-H., et al., *New Particle Formation in the Atmosphere: From Molecular Clusters to Global Climate.* Journal of Geophysical Research: Atmospheres, 2019. **124**(13): p. 7098-7146.
2. Kerminen, V.M., et al., *Atmospheric new particle formation and growth: review of field observations.* Environ. Res. Lett., 2018. **13**(10): p. 38.
3. Nilsson, E.D., et al., *Effects of continental boundary layer evolution, convection, turbulence and entrainment, on aerosol formation.* Tellus B: Chemical and Physical Meteorology, 2001. **53**(4): p. 441-461.
4. Nyeki, S., et al., *Condensation nuclei (CN) and ultrafine CN in the free troposphere to 12km: a case study over the Jungfraujoch high-alpine research station.* Geophys. Res. Lett., 1999. **26**: p. 2195-2198.
5. Kulmala, M., et al., *Analysis of the growth of nucleation mode particles observed in Boreal forest.* Tellus, 1998. **50**: p. 449-462.
6. Wehner, B., et al., *Observations of turbulence-induced new particle formation in the residual layer.* Atmos. Chem. Phys., 2010. **10**: p. 4319-4330.
7. Boulon, J.K., et al., *Investigation of nucleation events vertical extent: a long term study at two different altitude sites.* Atmos. Chem. Phys., 2011. **11**: p. 5625-5639.
8. Siebert, H., F. Stratmann, and B. Wehner, *First observations of increased ultrafine particle number concentrations near the inversion of a continental planetary boundary layer and its relation to ground-based measurements.* Geophysical Research Letters, 2004. **31**(9).
9. Lai, S., et al., *The striking effect of vertical mixing in the planetary boundary layer on new particle formation in the Yangtze River Delta.* Science of The Total Environment, 2022. **829**: p. 154607.
10. Wu, H., et al., *The impact of the atmospheric turbulence-development tendency on new particle formation: a common finding on three continents.* National Science Review, 2021. **8**(3).
11. Wang, J., et al., *Amazon boundary layer aerosol concentration sustained by vertical transport during rainfall.* Nature, 2016. **539**(7629): p. 416-419.
12. Fan, J.W., et al., *Substantial convection and precipitation enhancements by ultrafine aerosol particles.* Science, 2018. **359**(6374): p. 411-418.
13. Lampilahti, J., et al., *Aerosol particle formation in the upper residual layer.* Atmos. Chem. Phys., 2021. **21**(10): p. 7901-7915.
14. Liu, Y., et al., *Impact of residual layer transport on air pollution in Beijing, China.* Environmental Pollution, 2021. **271**: p. 116325.
15. Wang, Y., et al., *Sulfur Dioxide Transported From the Residual Layer Drives Atmospheric Nucleation During Haze Periods in Beijing.* Geophysical Research Letters, 2023. **50**(6): p. e2022GL100514.
16. Williamson, C.J., et al., *A large source of cloud condensation nuclei from new particle formation in the tropics.* Nature, 2019. **574**(7778): p. 399-403.
17. Chen, H., et al., *Vertically resolved concentration and liquid water content of atmospheric nanoparticles at the US DOE Southern Great Plains site.* Atmos. Chem. Phys., 2018. **18**: p. 311-326.

18. Meskhidze, N., et al., *Possible Wintertime Sources of Fine Particles in an Urban Environment.* Journal of Geophysical Research: Atmospheres, 2019. **124**(23): p. 13055-13070.
19. Kanawade, V., D.R. Benson, and S.H. Lee, *Statistical analysis of 4 year measurements of aerosol sizes in a semi-rural U.S. continental environment.* Atmos. Environ., 2012. **59**: p. 30-38.
20. Guenther, A., et al., *Estimates of global terrestrial isoprene emissions using MEGAN (Model of Emissions of Gases and Aerosols from Nature).* Atmos. Chem. Phys., 2006. **6**: p. 3181-3210.
21. Kalivitis, N., et al., *Atmospheric new particle formation as a source of CCN in the eastern Mediterranean marine boundary layer.* Atmos. Chem. Phys., 2015. **15**: p. 9203-9215.
22. Pöhlker, M.L., et al., *Aitken mode particles as CCN in aerosol- and updraft-sensitive regimes of cloud droplet formation.* Atmos. Chem. Phys., 2021. **21**(15): p. 11723-11740.
23. Brines, M., et al., *Traffic and nucleation events as main sources of ultrafine particles in high-insolation developed world cities.* Atmos. Chem. Phys., 2015. **15**(10): p. 5929-5945.
24. Hama, S.M.L., R.L. Cordell, and P.S. Monks, *Quantifying primary and secondary source contributions to ultrafine particles in the UK urban background.* Atmospheric Environment, 2017. **166**: p. 62-78.
25. Hofman, J., et al., *Ultrafine particles in four European urban environments: Results from a new continuous long-term monitoring network.* Atmospheric Environment, 2016. **136**: p. 68-81.
26. Saha, P.K., et al., *Reduced Ultrafine Particle Concentration in Urban Air: Changes in Nucleation and Anthropogenic Emissions.* Environmental Science & Technology, 2018. **52**(12): p. 6798-6806.
27. Rönkkö, T., et al., *Traffic is a major source of atmospheric nanocluster aerosol.* Proceedings of the National Academy of Sciences, 2017. **114**(29): p. 7549.
28. Guo, S., et al., *Remarkable nucleation and growth of ultrafine particles from vehicular exhaust.* Proceedings of the National Academy of Sciences, 2020. **117**(7): p. 3427.

22. Stull, R.B. *Transilient Turbulence Theory: A Nonlocal Description of Convection*. In: Plate, E.J., Fedorovich, E.E., Viegas, D.X., Wyngaard, J.C. (eds) *Buoyant Convection in Geophysical Flows*. NATO ASI Series, 1998, vol 513. Springer, Dordrecht.
23. Alabama Department of Transportation. *Alabama Traffic Data.* https://aldotgis.dot.state.al.us/TDMPublic/
24. Yu, H., Ortega, J., Smith, J. N., Guenther, A. B., Kanawade, V. P., You, Y., Liu, Y., Hosman, K., Karl, T., Seco, R., Geron, C., Pallardy, S. G., Gu, L., Mikkilä, J., and Lee, S-H: *New Particle Formation and Growth in an Isoprene-Dominated Ozark Forest: From Sub-5 nm to CCN-Active Sizes*, Aerosol Science and Technology, 2014. **48**:12, 1285-1298.
25. Zhang, S., Lyu, Y., Yang, X., Yuan, L., Wang, Y., Wang, L., Liang, Y., Qiao, Y., and Wang, S.: *Modeling Biogenic Volatile Organic Compoints Emissions and Subsequent Impacts on Ozone Air Quality in the Sichuan Basin, Southwestern China*. Front. Ecol. Evol., 2022. **10**.
26. Schmidt CW.: *Pollen Overload: Seasonal Allergies in a Changing Climate*. Environ Health Perspect., 2016. Apr;**124**(4):A70-5. doi: 10.1289/ehp.124-A70. PMID: 27035881; PMCID: PMC4829390.